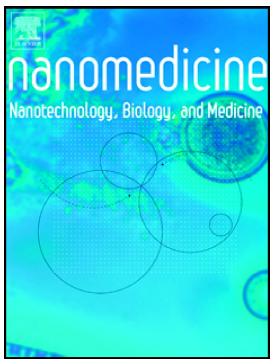

Ruthenium metallodendrimer against triple-negative breast cancer in mice

Sylwia Michlewska, Dagmara Wójkowska, Cezary Watala, Elżbieta Skiba, Paula Ortega, Francisco Javier de la Mata, Maria Bryszewska, Maksim Ionov

PII: S1549-9634(23)00054-0

DOI: https://doi.org/10.1016/j.nano.2023.102703

Reference: NANO 102703

To appear in: *Nanomedicine: Nanotechnology, Biology, and Medicine*

Revised date: 11 July 2023

Please cite this article as: S. Michlewska, D. Wójkowska, C. Watala, et al., Ruthenium metallodendrimer against triple-negative breast cancer in mice, *Nanomedicine: Nanotechnology, Biology, and Medicine* (2023), https://doi.org/10.1016/j.nano.2023.102703

Ruthenium metallodendrimer against triple-negative breast cancer in mice

Sylwia Michlewska[1,2]*, Dagmara Wójkowska[3], Cezary Watala[3], Elżbieta Skiba[4], Paula Ortega[5,6], Francisco Javier de la Mata[5,6], Maria Bryszewska[2], Maksim Ionov[2]

1 Laboratory of Microscopic Imaging and Specialized Biological Techniques, Faculty of Biology and Environmental Protection, University of Lodz, Poland.
2 Department of General Biophysics, Faculty of Biology and Environmental Protection, University of Lodz, Poland.
3 Department of Haemostatic Disorders, Faculty of Health Sciences, Medical University of Lodz, Poland.
4 Institute of General and Ecological Chemistry, Lodz University of Technology, Poland.
5 Universidad de Alcalá. Department of Organic and Inorganic Chemistry, and Research Institute in Chemistry "Andrés M. del Río" (IQAR), Madrid, Spain. Instituto de Investigación Sanitaria Ramón y Cajal, IRYCIS, Spain.
6 Networking Research Center on Bioengineering, Biomaterials and Nanomedicine (CIBER-BBN), Spain.

*Corresponding author, Sylwia Michlewska
e-mail: sylwia.michlewska@biol.uni.lodz.pl

Conflict of interest: The authors declare no conflict of interest

This work was co-financed by the project “Np-Hale” (Beethoven Life 1 program) No: 2018/31/F/NZ5/03454 granted by National Science Centre of Poland, project "NanoTENDO" under the M-ERA.NET 2 of Horizon 2020 programme, project No: 685451 granted by National Science Centre of Poland and funded by the grants from PID2020-112924RB-I00 (MINECO), consortiums IMMUNOTHERCAN-CM B2017/BMD-3733, NANODENDMED II-CM ref B2017/BMD-3703 and Project SBPLY/17/180501/000358 Junta de Comunidades de Castilla-La Mancha (JCCM). ERDF/ESF.

Abstract: 82 words
Complete manuscript: 4421 words
Number of references: 58
Number of tables: 1
Number of figures: 5

Abstract

Carbosilane metallodendrimers, based on the arene Ru(II) complex (**CRD13**) and integrated to imino-pyridine surface groups have been investigated as an anticancer agent in a mouse model with triple-negative breast cancer. The dendrimer entered into the cells efficiently, and exhibited selective toxicity for 4T1 cells. *In vivo* investigations proved that a local injection of

CRD13 caused a reduction of tumour mass and was non-toxic. ICP analyses indicated that Ru(II) accumulated in all tested tissues with a greater content detected in the tumour.

Keywords: Ruthenium metallodendrimer, anticancer agent, toxicity, tumour weight, *in vivo*.

1. Background

Breast cancer is one of the most common diseases in the female population worldwide. Presently, good preventative care, such as screening tests, increases the chances of survival, with the development of good diagnostics and new therapies which can prolong the lifetime of patients. Effective methods of breast cancer treatment include not only conventional surgery, chemotherapy and radiation, but also more directed approaches that rely on molecular targeted therapy and immunotherapy (1,2). As a result, the mortality rate of breast cancer has dropped considerably recently, especially in developing countries (3,4). Breast cancer can be diagnosed even in young women (1) and early recognition is crucial as the chance of survival is greater the sooner it is diagnosed and treated. However, frequently cancers are identified too late with the advanced stages of a primary tumour causing a problem and its metastases. The most common clinical subtypes of breast cancer are those associated with the oestrogen receptor (ER), the progesterone receptor (PR), the human epidermal growth factor receptor type 2 (HER2) and the so-called triple-negative (ER-/PR-/HER2) breast cancer. Amongst all breast cancers, the ER/PR+(hormone receptor) type accounts for over 60% of the cases, while the HER2+(HER2) subtype is of nearly 25%in occurrence (1,5). Triple-negative breast cancer (TNBC) (ER-/PR-/HER2) consists of approximately 15–20% of all diagnoses (6,7). TNBC is the most malignant subtype (1,6), characterized by a poor prognosis when compared to the hormonal receptor-positive and HER2-positive subtypes (6). Currently, chemotherapy is one of the most effective therapies for cancer (8,9). Unfortunately, most chemotherapeutics are poorly bioavailable and highly toxic to healthy tissues (10). It is also known that the ineffectiveness of cancer therapy is often dependent on drug resistance effects resulting from the rapid drug elimination from

cancer cells (11). Therefore, one of the main challenges for the development of new therapeutics is to find safe drugs which are able to target tumour cells and have an extended and prolonged effect in the tumour environment.

Currently, there has been focus on the field of nanotechnology. To reduce toxicity and increase the effect of anticancer drugs, different nanomaterials, such as liposomes (12), micelles (13), various polymeric materials (14,15), hydrogels (16) and dendrimers (17), have been studied as drug delivery agents. However, only a few nanoparticles have progressed to the clinical scale (18). In this context, dendrimers are in the spotlight, as effective and promising vehicles for drugs or genes (17,19–23). Controllable and precise synthesis, low immunogenicity and monodispersity make these spherical polymers useful in biomedicine (6,24–26). There are additional benefits of dendrimers in regard to their safety and reproducibility (26,27). Dendrimers have a well-defined and hyperbranched structure, making them excellent nano-vehicles for different kinds of biomolecules (19,28) and dendrimers complexed with drugs are able to increase drug selectivity, specificity, stability, and bioavailability (23,29). Dendrimers can be covalently modified by ligands or functional molecules (30) and it is possible to bind the anti-cancer metals, such as titanium, copper, or ruthenium to their surface groups to give them anti-cancer properties (24,25,31–34). Ruthenium compounds are in the spotlight of much research (3,19,35,36) as complexes of this metal seem to be a promising alternative for anticancer drugs based on cisplatinum. Currently, cisplatin derivatives are commonly used for the cancer treatment, especially for breast cancer (35), however they have a wide range of negative side effects (34,37,38). Ruthenium compounds demonstrate high activity against cancer *in vitro* and *in vivo* (17,34,39,40) and the ruthenium complexes RAPTA-C (41,42), NAMI-A, and KP1019 (43) have been intensively investigated in clinical and preclinical trials. The NAMI-A compound has been characterized as an efficient anti-metastatic drug (43).

Based on our previous *in vitro* results describing the effectiveness of the ruthenium dendrimer G_1-[[NCPh(*o*-N)Ru(η6-*p*-*cymene*)Cl]Cl]$_4$ (**CRD13**) against leukaemia and breast cancer, we tried to evaluate its *in vivo* activity with the triple negative breast cancer (TNBC)

model. Here we show that **CRD13** accumulates predominantly in tumour tissue with the dendrimer decreasing tumour growth but not influencing the condition of mice negatively. Based on the obtained results, the authors concluded that the ruthenium dendrimer **CRD13** could be suggested as an alternative drug/gene carrier for the therapy of triple-negative breast cancer.

2. Materials and methods

2.1. Dendrimers

The carbosilane ruthenium metallodendrimer of generation 1 with 4 imine-pyridine surface groups was considered as an anti-tumour agent. For the confocal microscopy studies its fluorescently labelled analogue ({[[NCPh(o-N)Ru(η6-p-cymene)Cl]Cl]3[FITC]} CRD13-FITC) was applied. Full biochemical and biophysical characteristics of G1-[[NCPh(o-N)Ru(η6-p-cymene)Cl]Cl]4 CRD13 and CRD13-FITC including the surface potential, morphology, haemocyto-toxicity and biological effects were reported previously (19,32,34). The structures of CRD13 and CRD13-FITC are shown in Figure 1.

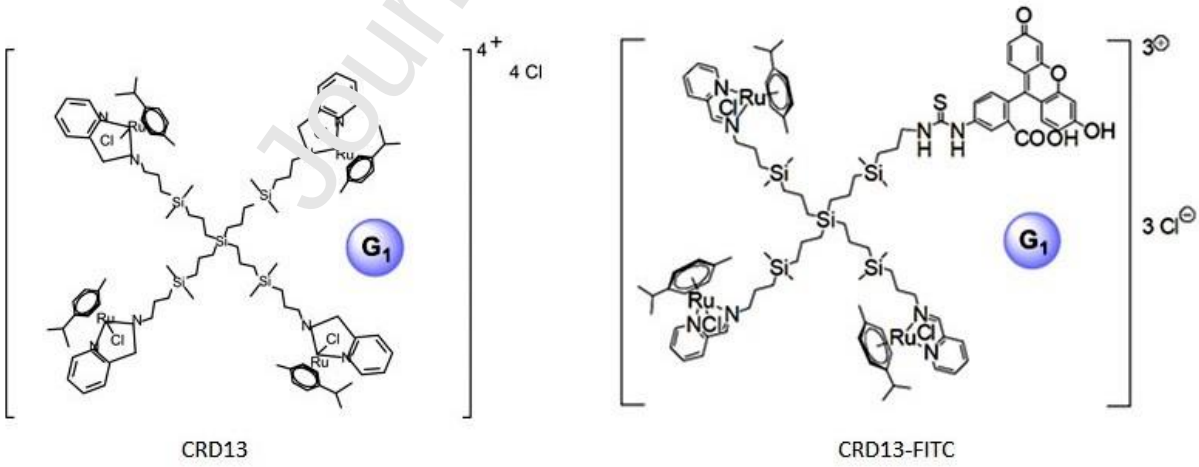

Figure 1. The structures of G1-[[NCPh(o-N)Ru(η6-p- cymene)Cl]Cl]4 (CRD13) and ({[[NCPh(o-N)Ru(η6-p-cymene)Cl]Cl]3[FITC]} (CRD13-FITC).

2.2. Cells (*in vitro*)

Normal EpH4-Ev (a mouse epithelial cell line) and 4T1 (a mouse breast cancer cell line), were purchased from ATCC (Manassas, Virginia, USA), and used to assess **CRD13** cytotoxicity. Cells were kept in plastic tissue culture flasks (Falcon, GE Healthcare Life Sciences, Chicago, Illinois, USA) in the RPMI-1640 (Gibco, Thermo Fisher Scientific, Waltham, MA, USA) and supplemented with 10% heat-inactivated foetal bovine serum (FBS, HyClone, GE Healthcare Life Sciences, Chicago, Illinois, USA)

2.3. Cytotoxicity (*in vitro*)

EpH4-Ev and 4T1 cells in the medium without FBS were seeded on 96-well black microtiter plates with a density of $3x10^4$/well. Cells were treated with the dendrimer in concentrations ranging from 2 to 20 µg/mL with the following incubation for 24 h and 72 h. The CellTiter-Blue® Assay (Promega Corporation, Madison, Wisconsin, USA) was used to evaluate cell viability that was calculated according to the equation:

$$\% \text{ viability} = (A/Ac) \times 100\ \%,$$

where: A - represents the fluorescence of the sample, Ac - is the fluorescence of the untreated control cells. The data were obtained in 3 independent repetitions used to fit the dose-response curve.

2.4. Internalization assay (*in vitro*)

Confocal microscopy technique was applied to analyse the internalization of **CRD13** into 4T1 cells. Cells suspended in RPMI-1640 at the count of 1×10^5 cells per well were seeded on 24-well plates with a glass bottom. After 24 h and 72h incubation with a dendrimer (10 and 20 µg/ml), cells were washed x2 with phosphate-buffered saline (PBS) and fixed with 4% formalin (20 min). After washing, 5 µg/mL 4′,6-diamidino-2-phenylindole) (DAPI) (Thermo Fisher Scientific, Waltham, MA, USA) was added to stain the nucleus. A Leica TCS SP8

confocal microscope (Leica Microsystems, Frankfurt, Germany) with a 63×/1.40 (HC PL APO CS2, Leica Microsystems) objective and different wavelength ranges (405 nm and 489 nm) was used to take confocal images. The Leica Application Suite X software (LAS X, Leica Microsystems, Frankfurt, Germany) was used for the data analysis. Fifty cells from each of 10 images were taken to the numerical analysis and the results are presented as a mean ± standard deviation (SD).

2.5. Mice and experimental design

8–12 weeks old female BALB/c mice were acquired from the Animal Facility of the University of Lodz, Poland and housed under standard conditions at the Animal House of the Medical University of Lodz (Lodz, Poland). All animals were weighed (≈18 g) and randomly allocated to 4 groups (5-15 mice per group). The experiments were performed under National Animal Care Committee regulations and were approved by the Local Ethical Committee for Animal Research in Lodz (license number 28/ŁB141/2019). To minimize animal suffering and reduce numbers (the 3Rs principle), we adapted the incomplete experimental design of the *in vivo* experiments. In the control groups, group 1 (not treated with **CRD 13**, not inoculated) and in group 2, (treated with **CRD13**, not inoculated with 4T1 cells) only 5 mice per group were planned. In groups 3 and 4 (treated with 4T1 cells and/or dendrimer) 15 animals per group were examined.

Group 1 were healthy mice treated by PBS only in appropriate volumes and was considered the control group (5 mice). Group 2 included the mice treated with **CRD13**, 10 mg/kg body weight (b.w.), every 2 days of a 28-day experiment (starting from day 2, 5 mice). Group 3 included the mice with tumours induced by the injection of 4T1 cells on the first day of the experiment (15 mice) (see section 2.6. for the details). Group 4 included the mice with tumours and injected with **CRD13**, 10 mg/kg b.w. every 2 days 28-day experiment (starting from day 2, 15 mice). The graphical presentation of the experimental scheme is given in Fig. 2.

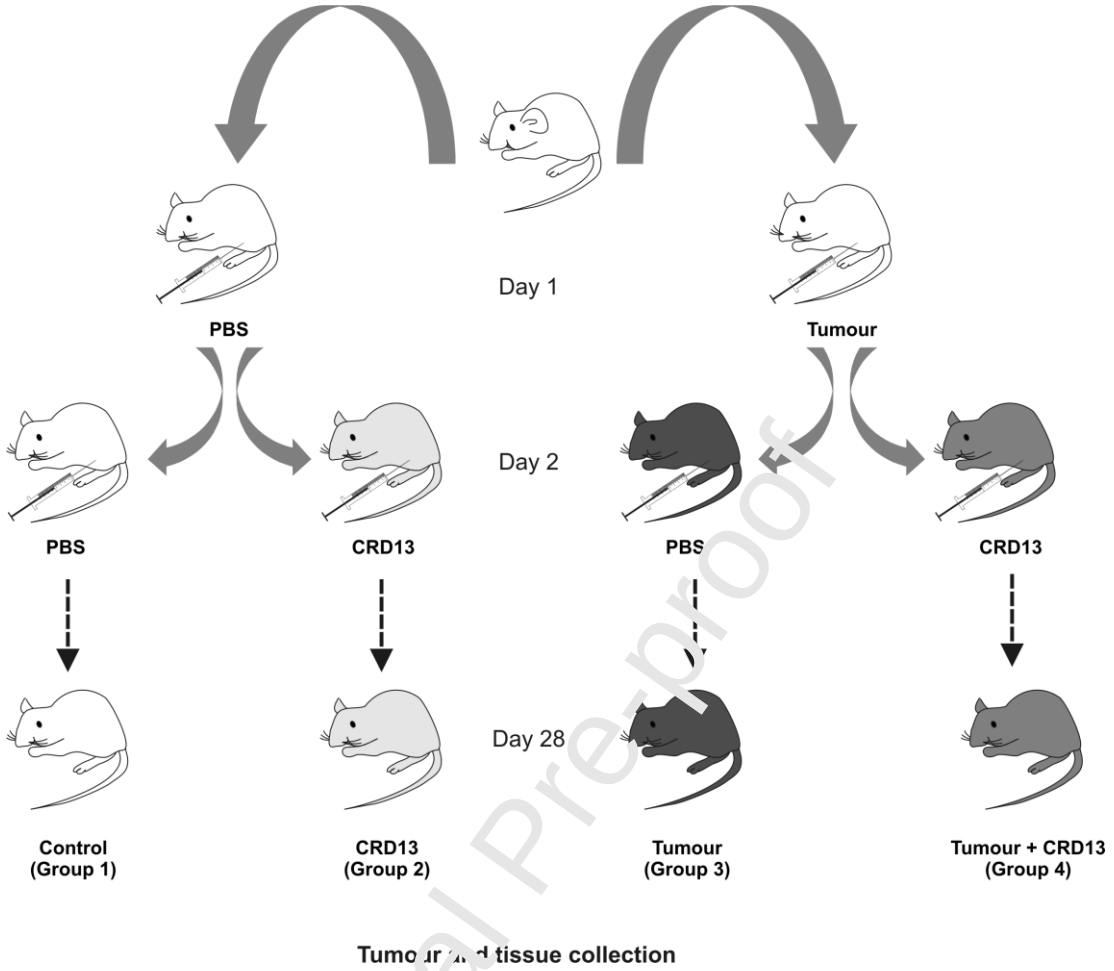

Figure 2. Scheme of the *in vivo* experimental design. Mice were randomly assigned to 4 independent groups. Mice were inoculated with cancer cells, and from day 2 were treated with **CRD 13** dendrimer for 26 days according to the scheme 2 x 2. Group 1 - NT (PBS), (not treated with **CRD13**, not inoculated with 4T1 cells), Group 2 - (treated with dendrimer every 2 days on the days 2.-28.), Group 3 - (cancer cells application), Group 4 - (inoculated with the cancer cells 4T1+ treatment with the dendrimer every 2 days on the days 2.-28.). Tumours and tissues were collected *post mortem* at day 28 of the experiment.

2.6. Induction of breast tumour in animals

4T1 cells (Murine breast cancer), purchased from the American Type Culture Collection, (ATCC), were cultured in RPMI-1640 with 10% foetal bovine serum (HyClone, GE

Healthcare Life Sciences, Chicago, USA) in standard flasks. After reaching 80% confluence, cells were harvested and a suspension at a cell count of 10^4 per 100 µl PBS per mouse was injected subcutaneously in the inguinal nipple area to induce the neoplasm. Subsequently, animals were treated with **CRD13** by subcutaneous injection every other day from day 2 to 28 of the experiment. Afterward, mice were sacrificed and their tumours and tissues were collected.

2.7. Tumour and organs weight

On Day-28 of the experiment, mice were anesthetized by an intraperitoneally application of xylazine (Biowet, Pulawy, Poland) in a dose of 20 mg/kg and ketamine (Biowet, Pulawy, Poland) in a dose of 100 mg/kg, weighed, and sacrificed by perfusion, next their tumours and organs (lungs, kidneys, and liver) were collected and weighed using laboratory scales.

2.8. Inductively Coupled Plasma (ICP)

Ruthenium determination was carried out by the Inductively Coupled Plasma Optical Emission Spectrometry method (ICP-OES). Firstly, weighted subsamples (0.3 g) of mice tissue were placed in a mixture of concentrated HNO_3 and HCl (6:1, w/w) using the Anton Paar Multiwave 3000 closed system instrument. Then samples were put in closed Teflon vessels, heated for 25 min. (10 min. of temperature ramp and 15 min. in stable conditions), and then cooled for 15 min. under the following operating parameters of the apparatus: magnetron power 1000 W, pressure 60 bar and temperature 240°C. After heating and cooling, samples were allowed to reach room temperature and diluted to a final volume of 25 mL with the mixture of HNO_3 and HCl prepared under the same conditions as for the blank sample. After processing, Ru was determined using the ICP-OES spectrometer PlasmaQuant PQ 9000 Elite, Analytik Jena (Jena, Germany). The calibration curve was produced by preparing of the following standard solutions: 0.02 $mg \cdot L^{-1}$; 0.05 $mg \cdot L^{-1}$ and 0.10 $mg \cdot L^{-1}$ in a highly pure 5% HNO_3 solution. The Limit of Detection and the Limit of

Quantification was 0.001 $mg \cdot L^{-1}$ and 0.004 $mg \cdot L^{-1}$, respectively. Operation parameters of the ICP-OES were as follows: wavelength - 240.272 nm, power - 1200 W, plasma gas flow rate - 12 $L \cdot min^{-1}$, auxiliary gas flow rate - 0.5 $L \cdot min^{-1}$, nebulizer gas flow rate - 0.5 $L \cdot min^{-1}$, read time - 9 s, delay time on sample injection - 15 s, pump speed - 1 $mL \cdot min^{-1}$, wash time: 15 s, number of replicates – 3.

2.9. Statistical analysis

Data were presented as the BCA bootstrap-boosted means ± SD or median with interquartile range (lower quartile [25 %] to upper quartile [75 %]), depending on data distribution). Data normality and variance homogeneity of the acquired data were verified using Shapiro–Wilk's or Levene's test, respectively. The data that complied with the assumptions of normal distribution and homogeneity of variances were analysed with the Student's t-test and one-way or two-way ANOVA, while for the remaining data were analysed with a Mann-Whitney rank sum U test and Kruskal-Wallis test. In order to assess the significance of differences between particular samples, the *post-hoc* multiple comparisons tests were used (the least significant difference test [LSD] or the Bonferroni's correction for multiple comparisons). In general, due to small sample sizes and the low statistical power of the estimated inferences in the majority of calculations the resampling bootstrap technique (10,000 iterations) was used as a routine to minimize the risk that the revealed differences were observed by pure chance; in such circumstances, we refer to the bootstrap-boosted test statistics instead of the classical approach. Statistical analyses were performed using Statistica v.13 (Dell Inc., Tulsa, OH), GraphPad Prism for Windows ver. 5.0 (GraphPad Software, San Diego, CA) and Resampling Stats Add-In for Excel v.4 (The Institute for Statistics Education, An Elder Research Company, Arlington, VA).

3. Results

3.1. Cytotoxicity assay (*in vitro*)

The cytotoxicity of **CRD13** was tested using mouse EpH4-Ev and 4T1 (murine breast cancer) cell lines, incubated with the dendrimer for 24 or 72 h. The results indicated that **CRD13** was more cytotoxic towards cancer (4T1) than normal cells (EpH4-Ev), this effect being time- and concentration-dependent. The viability of EpH4-Ev in the presence of **CRD13** was not significantly different compared to the untreated, control cells (incubation 24 h), while in the case of 4T1 cells the viability was decreased by up to 50 % (Fig. 3A). With an increase of the incubation time up to 72 h, a gradually decreased number of living EpH4-Ev cells, down to about 45% of control was observed, whereas the viability of cancer cells dropped by more than 90 % at the highest applied dendrimer concentration of 20 µg/ml (Fig. 3B).

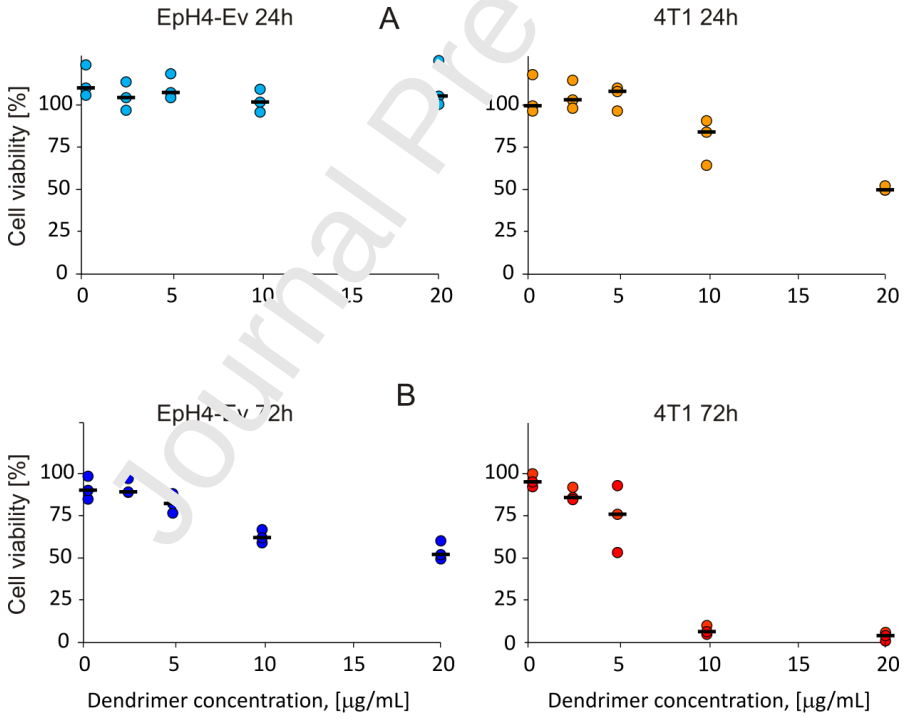

Figure 3. Viability of EpH4-Ev and 4T1 cells exposed to ruthenium dendrimer **CRD13**. (**A**) – incubation time 24 h, (**B**) – incubation time 72 h. Data, acquired with the use of fluorescence technique, are presented as relative values vs. control samples. Results are shown as raw estimates, means are represented by thick horizontal lines; each point represents the mean of 3 technical

replicates of the sample. The significance of differences, as estimated with the bootstrap-boosted two-way ANOVA, was as follows: for EpH4-Ev, the effect of time $P< 0.0001$, for **CRD13** concentration, $P< 0.001$, for the interaction of factors, $P< 0.003$; for 4T1 cells, the effects of time and **CRD13** concentration $P< 0.0001$, for the interaction of factors, $P< 0.001$.

Table 1. Inhibition concentrations IC50±SD (μg/ml) resulting in 50% dendrimer-mediated reduction of EpH4-Ev and 4T1 cell viability after 24 h and 72h of incubation.

	EpH4-Ev	4T1
24h	106.64±20.63	23.17±2.31
72h	21.48±3.00	9.99±1.20

3.2. Internalization assay

Confocal microscopy was applied to evaluate the ability of FITC labelled **CRD13** to internalize into 4T1 cells. The cellular uptake of dendrimer depended on its concentration (10 or 20 μg/ml) and incubation time (24 or 72 h). On average, the incubation of cells with the dendrimer for 24h lead to its internalization into 5.7 % (10 μg/ml) and 7.5 % (20 μg/ml) of cells. Extension of the incubation time up to 72 h increased the amount of the internalized agent by up to 10 % and 20 %, respectively, for the **CRD13** concentrations of 10 and 20 μg/ml (Fig. 4A,B). The highest values of general fluorescence intensity of the studied cells were observed for the samples containing **CRD13** in the concentration of 20 μg/ml, incubated for 72 h (Fig. 4A,C).

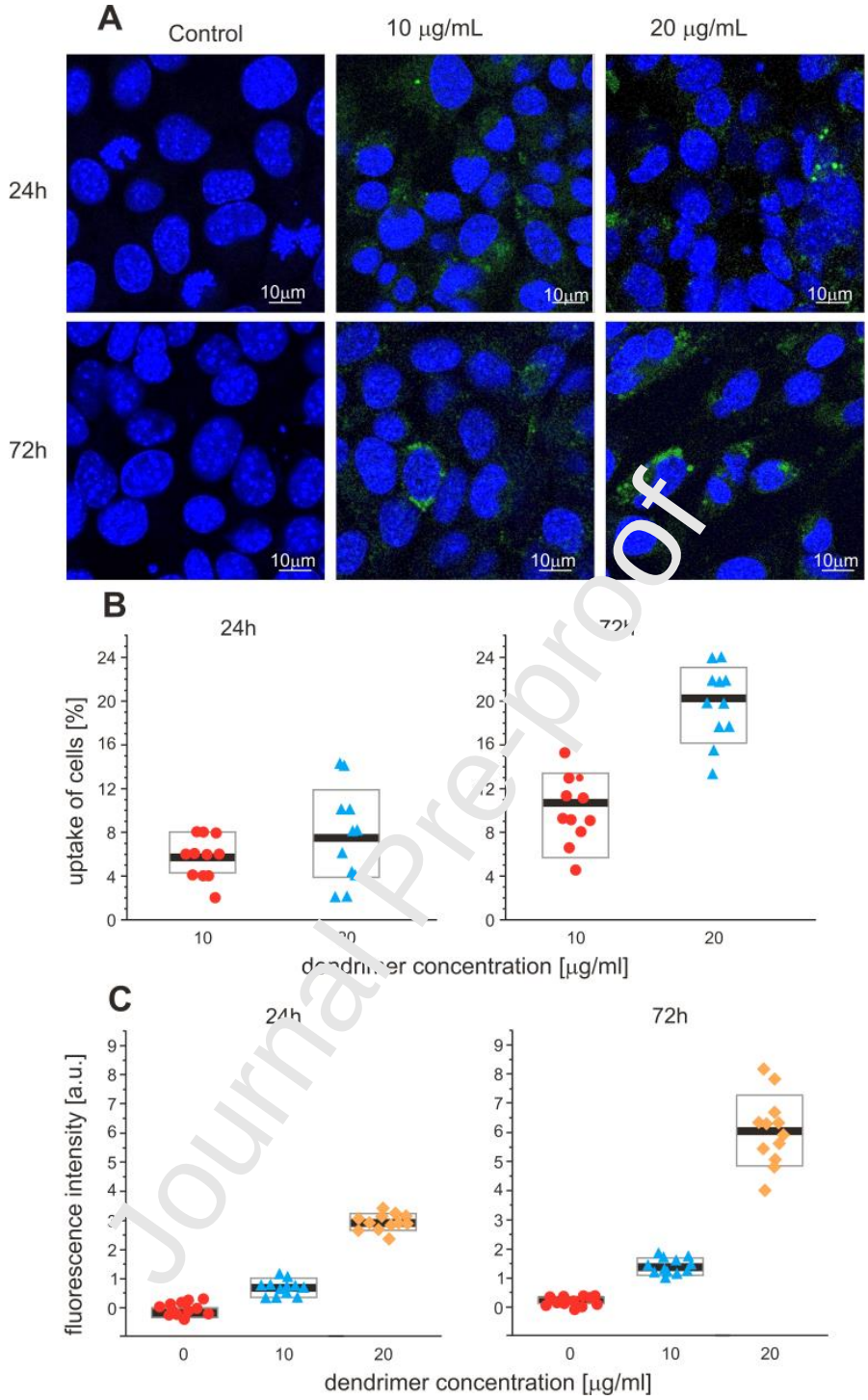

Figure 4. Cellular uptake of the FITC-labelled **CRD13**. (**A**) confocal microscopy images; microphotographs taken at λ_{em}=405 and 489 nm, (**B**) fractions of 4T1 cells uptaking **CRD13-FITC**; for the dendrimer concentrations of 10 μg/ml and 20 μg/ml the fractions of labelled cells were, respectively: 5.46+1.21% and 7.46+2.41% for 24 h incubation, and 10.27±2.13% and 19.64+1.86% for 72 h incubation; the significance by the bootstrap-boosted two-way ANOVA was: for the effects of time

and **CRD13** concentration *P*< 0.0001, for the interaction between the factors *P*< 0.001, (**C**) overall fluorescence intensity of **CRD13-FITC** internalized into the dendrimer-treated cells; for the dendrimer concentrations of 0, 10 μg/ml and 20 μg/ml the fractions of labelled cells were, respectively: 0.183±0.038 a.u., 1.354±0.147 a.u. and 6.309±0.693 a.u; significance by the bootstrap-boosted two-way ANOVA was P< 0.0001 for the effects of time, **CRD13** concentration and the interaction between the factors. The results are shown as the BCA bootstrap-boosted means ± SD of n = 11 (**B**) or n = 12 observations(**C**).

3.3. Tumour and organs weight

The effect of **CRD13** on mouse weight was assessed during the 28 days (see section 2.5. and 2.7. for details). The mass of the tumours, spleens and livers were analysed *post mortem* on the last day of the experiment. The weight of mice in all treatment groups did not change during the experiment (Fig. 5A). However, the evaluation of mean tumour weights (on day-28) indicated that the application of **CRD13** significantly decreased the tumour size (Fig. 6A,C) and overall weight (Fig. 6B) from about 0.89±0.21 mg to about 0.47±0.16 mg. In the mouse group untreated with the dendrimer, the tumour represented about 4.97 % of the total body mass on average and in the group of treated animals, the tumour represented on average only 2.43 % of the total body mass (Fig. 5B).

The spleen weights and sizes of the mice in all experimental groups were analysed.(Fig. 5C). In healthy animals, the administration of the dendrimer did not affect the size of the spleen (Fig. 6D). In the healthy (untreated) and dendrimer-treated mice, the spleen weight remained at a level of 0.07 mg consisting on average of about 0.40 % of the total body weight.

A visible increase in the size and weight of the spleen was observed in animals with the developed tumour. The average weight of the spleen increased from 0.07 mg to about 0.42 mg, which accounted for approximately 2.32 % of the mouse body mass. The application of the dendrimer resulted in a reduction of the spleen weight to ~ 0.25 mg, i.e. ~ 1.42 % of the whole body mass (Fig. 6E).

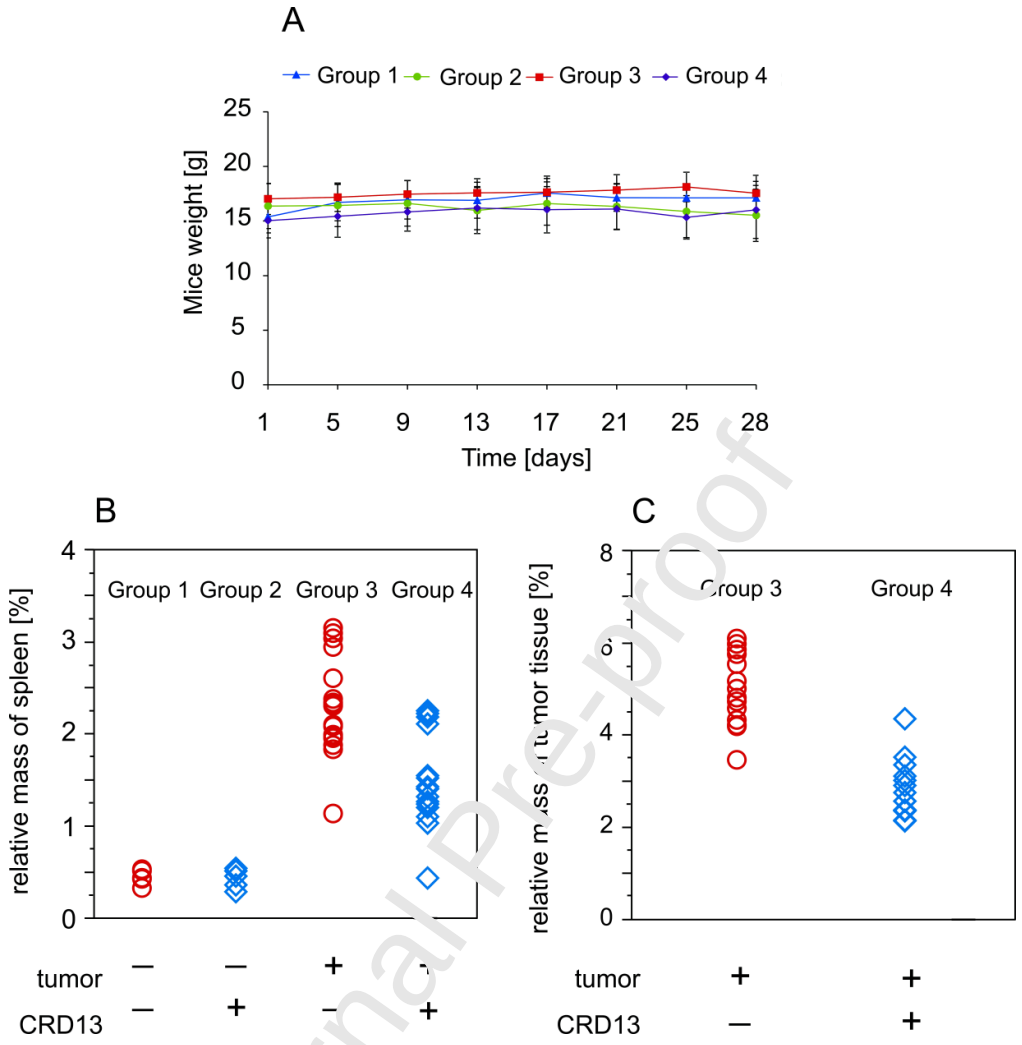

Figure 5. Body and tumour weights. (**A**) The impact of 28-day mice treatment with ruthenium dendrimer on body mass, (**B**) relative mass of the tumour tissue; significance for the relative tumour weight, estimated with the bootstrap-boosted Student t test was $P< 0.0001$, (**C**) the relative spleen weight (spleen mass/ total body mass ratio) of mice; significance, estimated with the bootstrap-boosted two-way ANOVA, was: the effect of the inoculation with 4T1 cells, $P< 0.0001$, for **CRD13** treatment, $P< 0.02$, for the interaction between factors, $P< 0.025$. Dendrimer was applied at the concentration of 10 mg/kg b.w. every day (days 2-28); n = 5 (groups 1 and 2), n = 15 (groups 3 and 4).

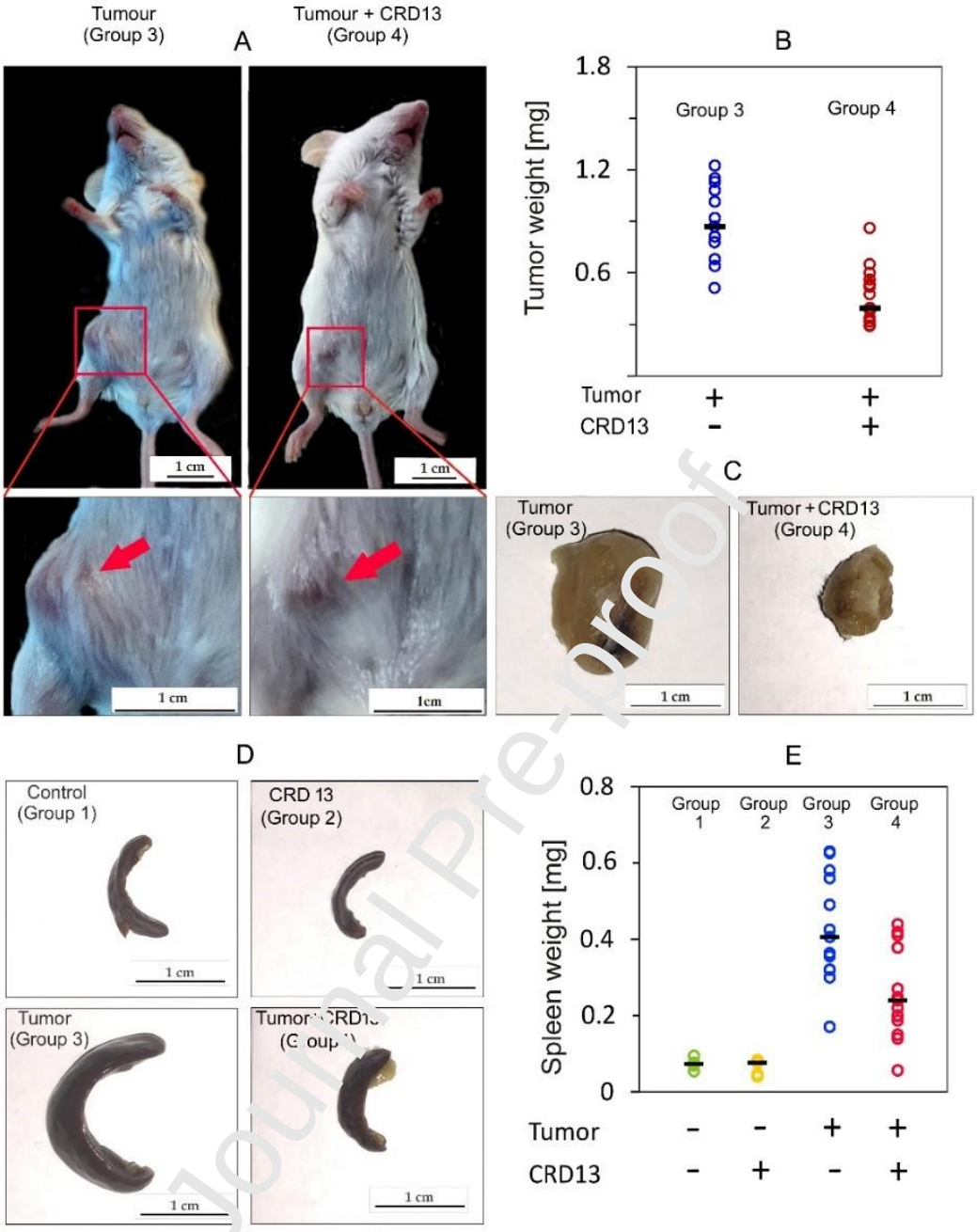

Figure 6. Changes of the tumour and spleen weight in mice treated with **CRD13**. (**A**) Tumour images of animals treated or untreated with ruthenium dendrimer **CRD13**. (**B**) tumour weight [mg], thick black horizontal lines stand for means; significance, significance by bootstrap-boosted Student t test, P< 0.0001, (**C**) Photographs demonstrating the changes in tumour size under the influence of **CRD13**, (**D**) Spleen images of healthy mice and animals with cancer treated or untreated with **CRD13**, (**E**) spleen weight [mg] in healthy and diseased mice under the influence of **CRD13**; thick black horizontal lines stand for the means; significance by the bootstrap-boosted two-way ANOVA: the effect of inoculation with 1T4 cells, *P*<0.0001, the effect of **CRD13**, *P*< 0.0.04. The dendrimer was applied at the concentration of 10 mg/kg b.w. every 2 days (days 2-28). Group 1 - healthy mice treated with PBS

only (control), Group 2 – mice treated with dendrimer, Group 3 – mice inoculated with cancer cells at the day 1 of the experiment, Group 4 – mice applied with cancer cells at the day 1, and treated with the dendrimer every 2 days on the days 2-28 of the experiment. n = 5 for groups 1 and 2, n = 15 for groups 3 and 4.

3.4. Inductively Coupled Plasma (ICP).

The ICP technique was applied to analyse the biodistribution of ruthenium in different tissues of tested mice. Mouse organs for the ISP test were collected after 28 days of the experiment and ruthenium was found in all the collected tissues of animals treated with **CRD13**, with the content varying depending on the type of tissue. The greatest amount of ruthenium was accumulated in tumour tissue, about 48.02±3.85 μg g^{-1} (Tab. 2). Less amount of the metal were found in liver and kidney tissues, 12.34±4.28 μg g^{-1} and 8.41±2.89 μg g^{-1}, respectively. The smallest amounts of ruthenium (1.89±0.10 μg g^{-1}) were deposited in the lung tissue of mice in experimental group 4. Similar ruthenium contents were found in the tissues of mice in group 2, which were treated with dendrimer only. In this experimental group, ruthenium accumulated in the liver, kidney and lung in the concentrations of 10.13±0.19, 5.68±0.09 and 1.73±0.15 μg g^{-1}, respectively (Tab. 2).

Table 2. Ruthenium content in the selected organs of mice [μg·g^{-1}].

	Group 2 CRD13	Group 3 4T1	Group 4 4T1 + CRD13
Tumour	-	0.00	48.02±3.85
Lung	1.73±0.15	0.01±0.01	1.89±0.10#
Kidney	5.68±0.09	0.00	8.41±2.89*

Liver	10.13±0.19	0.00	12.34±4.26[##]

*The data are BCA bootstrap-boosted means ± SD of four independent samples (3 scans were made for each sample). Significance estimated with the bootstrap-boosted Student t test: [#]P=0.074, *P<0.02, [##]P=0.121, for tumour P<0.002.*

4. Discussion

Amongst breast cancers, triple-negative breast cancer (TNBC) is the most difficult to treat with the life expectancy of patients being significantly shorter than for other types (44). Moreover, TNBC is diagnosed in relatively young patients (45). The subtypes of this tumour are characterized by a higher aggressiveness and increased ability to form metastases (46). It is known that TNBC is sensitive to chemotherapy in the initial phase of treatment, but therapies for this type of cancer do not guarantee success and the risk of a recurrence in the following years is extremely high (45,46). Therefore it is important to find an alternative approach which will be selective and toxic for cancer, will concentrate on the reduction of tumour mass with no overall adverse effects and limited side effects (45).

Based on our previous results we concluded that the carbosilane ruthenium dendrimer **CRD13** can be effective against other types of cancers (25,30,32,47,48) and here we showed that this dendrimer could be useful in TNBC treatment. The cytotoxicity of **CRD13** towards normal EpH4-Ev (mouse epithelial) and 4T1 (mouse breast cancer) cells was evaluated. **CRD13** was more cytotoxic towards cancer than to normal cells. Obtained data were in good agreement with previously results, where the cytotoxic effect of **CRD13** was checked against PBMC (normal) and 1301 or HL-60 (leukaemia) cells (22,25,47).

The cytotoxicity of cationic dendrimers is generation- and concentration-dependent (33,49). This effect has been observed earlier for PAMAM, carbosilane, phosphorus dendrimers (49,50) and metallodendrimers containing ruthenium atoms (19,32) towards different cell

lines. Numerous studies focus on different ruthenium compounds as alternatives for cisplatinum-based drugs as ruthenium induces DNA damage (25,47,51–53). This metal, due to its similarities to iron, is taken up better by cancer than in normal cells (26,42,48). The ability of **CRD13** to internalize the 4T1 (murine breast cancer) cells was checked. The dendrimer was efficiently taken up by cells with internalization dependent on incubation time and concentration. Extension of the incubation time from 24 to 72 h not only increased the number of internalized cells, but also the number of nanoparticles inside cells. **CRD13** is positively charged, therefore it can interact with the negatively charged cell membrane, with the presence of ruthenium atoms probably helping to direct these nanoparticles towards cancer cells. A similar effect of **CRD13-FITC** was described earlier for leukaemia (34) and prostate cancer cells (30). Other studies using complexes formed by ruthenium metallodenrimers and nucleic acids showed that they can easily enter cancer cells (19).

An attempt to answer the question whether ruthenium dendrimer can be effective *in vivo* against TNBC was attempted here. As a simple evaluation parameter, the analysis of tumour and spleen weight was chosen for the preliminary estimation of **CRD13** effects. Experimental animals were divided into 4 groups as described in section 2.6., and animal/organ weight was analysed after treatment of the murine breast cancer cells with ruthenium dendrimer administration. The results obtained from experimental group 2 (**CRD13** only) show that the dendrimer did not influence the weight of the animal. Similar results have been found previously for animals with a model prostate cancer, where a 40-day treatment with **CRD13** produced no changes in the weight of mice, and indicated a low toxicity of the ruthenium dendrimer *in vivo* (30).

Our results show shrinking of the tumour weight after treatment with **CRD13**, with the relative weight of tumour tissue vs. body mass reduced from ~4.97 % (tumour) to ~2.4 % (tumor+**CRD13**). A similar impact of ruthenium metallodendrimers (30) and dendrons (54) has been noted for prostate tumours in *ex-vivo* and *in-vivo* models previously. The Ru metallodendrons exhibited anti-metastatic activity by hindering the adhesion of cells and inhibiting cell migration. Other Ru complexes, such as RAPTAC, decreased colorectal

cancer masses by half after 11 days of treatment (41). However, this complex was used at a higher concentration of 100 mg/kg/day, while in this study, the **CRD13** dendrimer was applied at the concentration of 10 mg/kg of body weight every second day.

An important side effect in mice with TNBC is splenomegaly (55–59). Enlargement of the spleen is usually the result of tumour involvement and infiltration of MDSCs (Myeloid-derived suppressor cells) into the spleen (56,59). MDSC's are heterogeneous immune cells from bone marrow stem cells and their presence in tissues supresses immunity, inducing an overactive spleen to provide tumour growth (56–58). For this reason, the weight of the mice's spleen was evaluated in all experimental groups in this study. The results showed that firstly the dose of metallodendrimer **CDR13** into healthy mice had no effect on the size of the liver and secondly in the case of the mice whose tumor had been induced, treatment with **CDR13** produced a significant reduction in the weight of the spleen compared to the control, which showed splenomegaly.

Finally, biodistribution of Ru(II) in mice tissues was assessed by the ICP method after the **CRD13** application, since it is extremely important to determine where the cytotoxic agent accumulates in order to control any side effects. As expected, the highest amount of metal was accumulated in the tumour, as also found in previous prostate cancer trials (30). The evaluation of other organs where accumulations were significantly lower, indicated selectivity of ruthenium metallodendrimers towards neoplastic tissue and so they seem to be relatively safe for animals. In view of these results, and the previous results obtained by ICP in the treatment of prostate cancer with these metallodendrimers, we can assume that any excess of ruthenium can be removed via the urine or faecal route (22,30).

5. Conclusions

All the results obtained in this work can be considered as a proof of concept for the use of dendrimer G_1-[[NCPh(*o*-N)Ru(η^6-*p*- *cymene*)Cl]Cl]$_4$ **CRD13** as an antitumor agent against the triple negative breast cancer mice model. The results open the door for the study of CRD13

in combined therapy with the aim of fighting this type of cancer in a less invasive way.

CRediT authorship contribution statement

S.M. Conceptualization, Data curation, Formal analysis, Methodology, Investigation, Visualization, Writing - original draft, Writing review & editing, **D.W.** Methodology, Investigation, **C.W.** Writing - review & editing, Methodology, Software, Data curation, Formal analysis, **E.S.** Methodology, Investigation, **P.O.** Writing - review & editing, Sources, **F.J.M.** Writing - review & editing, Sources, **M.B.** Funding acquisition, Data curation, Writing - review & editing, **M.I.** Conceptualization, Writing - review & editing, Project administration, Data curation, Formal analysis, Supervision

Compliance with ethical standards

All the experiments published in this manuscript comply with the current laws of the country in which they were performed. All institutional and national guidelines for the care and use of laboratory animals were followed. The procedures performed in current studies were in accordance with the ethical standards of National Animal Care Committee regulations, approved by the Local Ethical Committee for Animal Research in Lodz, Poland (license number ŁB141/2019). We respected 3R rules to minimize animal suffering.

Acknowledgments

The authors wish to thank Magda Gapińska from the Laboratory of Microscopic Imaging & Specialized Biological Techniques, Faculty of Biology & Environmental Protection, University

of Lodz for her technical assistance. We also acknowledge the UK English native speaker (BioMedES. co.uk) for the support in language correction.

References

1. Ngamcherdtrakul W, Yantasee W. siRNA therapeutics for breast cancer: recent efforts in targeting metastasis, drug resistance, and immune evasion. Transl Res. 2019;214:105–20.
2. Weinstein IB, Joe A. Oncogene addiction. Cancer Res. 2008;68(9):3077–80.
3. Golbaghi G, Castonguay A. Rationally designed ruthenium complexes for breast cancer therapy. Molecules. 2020;25(2).
4. Kumar A, Singla A. Epidemiology of Breast Cancer: Current Figures and Trends BT - Preventive Oncology for the Gynecologist. In: Mehta S, Singla A, editors. Singapore: Springer Singapore; 2019. p. 335–9.
5. D'Souza A, Spicer D, Lu J. Overcoming endocrine resistance in metastatic hormone receptor-positive breast cancer. J Hematol Oncol. 2018;11(1):1–10.
6. Liu M, Song W, Huang L. Drug delivery systems targeting tumor-associated fibroblasts for cancer immunotherapy. Cancer Lett. 2019;448:31–9.
7. Bray F, Ferlay J, Soerjomataram I, Siegel RL, Torre LA, Jemal A. Global cancer statistics 2018: GLOBOCAN estimates of incidence and mortality worldwide for 36 cancers in 185 countries. CA Cancer J Clin. 2018;68(6):394–424.
8. Bourgeois-Daigneault MC, Roy DG, Aitken AS, El Sayes N, Martin NT, Varette O, et al. Neoadjuvant oncolytic virotherapy before surgery sensitizes triple-negative breast cancer to immune checkpoint therapy. Sci Transl Med. 2018;10(422).
9. Weisman PS, Ng CKY, Brogi E, Eisenberg RE, Won HH, Piscuoglio S, et al. Genetic alterations of triple negative breast cancer by targeted next-generation sequencing and correlation with tumor morphology. Mod Pathol. 2016;29(5):476–88.
10. Zhang Y, Lu Y, Zhang Y, He X, Chen Q, Liu L, et al. Tumor-Targeting Micelles Based

on Linear-Dendritic PEG-PTX8 Conjugate for Triple Negative Breast Cancer Therapy. Mol Pharm. 2017;14(10):3409–21.

11. Abedi-Gaballu F, Dehghan G, Ghaffari M, Yekta R, Abbaspour-Ravasjani S, Baradaran B, et al. PAMAM dendrimers as efficient drug and gene delivery nanosystems for cancer therapy. Appl Mater Today. 2018;12:177–90.
12. Shen J, Kim H, Wolfram J, Mu C, Zhang W, Liu H, et al. Communication A Liposome Encapsulated Ruthenium Polypyridine Complex as a Theranostic Platform for Triple Negative Breast Cancer A Liposome Encapsulated Ruthenium Polypyridine Complex as a Theranostic Platform Research Center for Health and Nutrition , Sh. 2017;17(5):2913–20.
13. Liu Y, Zhou C, Wang W, Yang J, Wang H, Hong W, et al. CD44 Receptor Targeting and Endosomal pH-Sensitive Dual Functional Hyaluronic Acid Micelles for Intracellular Paclitaxel Delivery. Mol Pharm. 2016;13(12):4209–21.
14. Bowerman CJ, Byrne JD, Chu KS, Schorzman AN, Keeler AW, Sherwood CA, et al. Docetaxel-Loaded PLGA Nanoparticles Improve Efficacy in Taxane-Resistant Triple-Negative Breast Cancer. Nano Lett. 2017 Jan 11;17(1):242–8.
15. Kubczak M, Michlewska S, Bryszewska M, Aigner A, Ionov M. Nanoparticles for local delivery of siRNA in lung therapy. Adv Drug Deliv Rev. 2021;179:114038.
16. Zhang H, Liu XL, Zhang YF, Gao F, Li GL, He Y, et al. Magnetic nanoparticles based cancer therapy: current status and applications. Sci China Life Sci. 2018;61(4):400–14.
17. Michlewska S, Maroto M, Hołota M, Kubczak M, Sanz Del Olmo N, Ortega P, et al. Combined therapy of ruthenium dendrimers and anti-cancer drugs against human leukemic cells. Dalt Trans. 2021;50(27):9500–11.
18. Shi J, Kantoff PW, Wooster R, Farokhzad OC. Cancer nanomedicine: progress, challenges and opportunities. Nat Rev Cancer. 2017 Jan 11;17(1):20–37.
19. Michlewska S, Ionov M, Maroto-Díaz M, Szwed A, Ihnatsyeu-Kachan A, Loznikova S, et al. Ruthenium dendrimers as carriers for anticancer siRNA. J Inorg Biochem.

2018;181(2017):18–27.

20. Ionov M, Lazniewska J, Dzmitruk V, Halets I, Loznikova S, Novopashina D, et al. Anticancer siRNA cocktails as a novel tool to treat cancer cells. Part (A). Mechanisms of interaction. Int J Pharm. 2015;485(1–2):261–9.
21. Dzmitruk V, Szulc A, Shcharbin D, Janaszewska A, Shcharbina N, Lazniewska J, et al. Anticancer siRNA cocktails as a novel tool to treat cancer cells. Part (B). Efficiency of pharmacological action. Int J Pharm. 2015;485(1–2):288–94.
22. Michlewska S, Maly M, Wójkowska D, Karolczak K, Skiba E, Hołota M, et al. Carbosilane ruthenium metallodendrimer as alternative anti-cancer drug carrier in triple negative breast cancer mouse model: a preliminary study. Int J Pharm. 2023;122784.
23. Hołota M, Michlewska S, Garcia-gallego S, Sanz N, Ortega P, Bryszewska M, et al. Combination of Copper Metallodendrimers with Conventional Antitumor Drugs to Combat Cancer in In Vitro Models. 2023;
24. Hołota M, Magiera J, Michlewska S, Kubczak M, Olmo NSD, García-Gallego S, et al. In vitro anticancer properties of copper metallodendrimers. Biomolecules. 2019;9(4).
25. Michlewska S, Ionov M, Maroto-Díaz M, Szwed A, Ihnatsyeu-Kachan A, Abashkin V, et al. Ruthenium dendrimers against acute promyelocytic leukemia: In vitro studies on HL-60 cells. Future Med Chem. 2019;11(14).
26. Gouveia M, Figueira J, Jardim MG, Castro R, Tomás H, Rissanen K, et al. Poly(alkylidenimine) dendrimers functionalized with the organometallicmoiety [Ru(v 5-C5H5)(PPh3)2]+ as promising drugs against cisplatin-resistant cancer cells and humanmesenchymal stem cells. Molecules. 2018;23(6):1–17.
27. Grodzicka M, Pena-Gonzalez CE, Ortega P, Michlewska S, Lozano R, Bryszewska M, et al. Heterofunctionalized polyphenolic dendrimers decorated with caffeic acid: Synthesis, characterization and antioxidant activity. Sustain Mater Technol. 2022;33(September):e00497.
28. Białkowska K, Miłowska K, Michlewska S, Sokołowska P, Komorowski P, Lozano-Cruz

T, et al. Interaction of cationic carbosilane dendrimers and their siRNA complexes with MCF-7 cells. Int J Mol Sci. 2021;22(13).

29. Kesharwani P, Jain K, Jain NK. Dendrimer as nanocarrier for drug delivery. Prog Polym Sci. 2014;39(2):268–307.

30. Maroto-Diaz M, Sanz del Olmo N, Muñoz-Moreno L, Bajo AM, Carmena MJ, Gómez R, et al. In vitro and in vivo evaluation of first-generation carbosilane arene Ru(II)-metallodendrimers in advanced prostate cancer. Eur Polym J. 2019;113(January):229–35.

31. Katir N, Marcotte N, Michlewska S, Ionov M, El Brahmi N, Bousmina M, et al. Dendrimer for Templating the Growth of Porous Catechol-Coordinated Titanium Dioxide Frameworks: Toward Hemocompatible Nanomaterials. ACS Appl Nano Mater. 2019;2(5).

32. Maroto-Díaz M, Elie BT, Gómez-Sal P, Perez-Serrano J, Gómez R, Contel M, et al. Synthesis and anticancer activity of carbosilane metallodendrimers based on arene ruthenium(ii) complexes. Dalt Trans. 2016;45(16):7049–66.

33. Michlewska S, Ionov M, Shcharbin D, Maroto-Díaz M, Gomez Ramirez R, Javier de la Mata F, et al. Ruthenium metallodendrimers with anticancer potential in an acute promyelocytic leukemia cell line (HL60). Eur Polym J. 2017;87:39–47.

34. Michlewska S, Kubczak M, Maroto-Díaz M, Del Olmo NS, Ortega P, Shcharbin D, et al. Synthesis and characterization of FITC labelled ruthenium dendrimer as a prospective anticancer drug. Biomolecules. 2019;9(9).

35. Sanz N, Bajo AM, Ionov M, Garcia-gallego S, Gómez R, Ortega P, et al. Cyclopentadienyl ruthenium(II) carbosilane metallodendrimers as a promising treatment against advanced prostate cancer. Eur J Med Chem. 2020;199(Ii):112414.

36. Rodríguez-Prieto T, Michlewska S, Hołota M, Ionov M, de la Mata FJ, Cano J, et al. Organometallic dendrimers based on Ruthenium(II) N-heterocyclic carbenes and their implication as delivery systems of anticancer small interfering RNA. J Inorg Biochem. 2021;223:111540.

37. Llamazares C, Del Olmo NS, Ortega P, Gómez R, Soliveri J, Javier De La Mata F, et al. Antibacterial effect of carbosilane metallodendrimers in planktonic cells of gram-positive and gram-negative bacteria and staphylococcus aureus biofilm. Biomolecules. 2019;9(9):1–11.

38. Perisé-Barrios AJ, Jiménez JL, D'Omínguez-Soto A, De La Mata FJ, Corbí AL, Gomez R, et al. Carbosilane dendrimers as gene delivery agents for the treatment of HIV infection. J Control Release. 2014;184(1):51–7.

39. Jain K, Kesharwani P, Gupta U, Jain NK. Dendrimer toxicity: Let's meet the challenge. Int J Pharm. 2010;394(1–2):122–42.

40. Fröhlich E. The role of surface charge in cellular uptake and cytotoxicity of medical nanoparticles. Int J Nanomedicine. 2012;7:5577–91.

41. Weiss A, Berndsen RH, Dubois M, Müller C, Schibli R, Griffioen AW, et al. In vivo anti-tumor activity of the organometallic ruthenium(ii)-arene complex [Ru(η6-p-cymene)Cl2(pta)] (RAPTA-C) in human ovarian and colorectal carcinomas. Chem Sci. 2014;5(12):4742–8.

42. Govender P, Sudding LC, Clavel CM, Dyson PJ, Therrien B, Smith GS. The influence of RAPTA moieties on the antiproliferative activity of peripheral-functionalised poly(salicylaldiminato) metallodendrimers. Dalt Trans. 2013;42(4):1267–77.

43. Alessio E, Messori L. NAMI-A and KP1019/1339, Two Iconic Ruthenium Anticancer Drug Candidates Face-to-Face: A Case Story in Medicinal Inorganic Chemistry. Molecules. 2019;24(10):1–20.

44. Lin NU, Vanderplas A, Hughes ME, Theriault RL, Edge SB, Wong YN, et al. Clinicopathologic features, patterns of recurrence, and survival among women with triple-negative breast cancer in the National Comprehensive Cancer Network. Cancer. 2012;118(22):5463–72.

45. Boyle P. Triple-negative breast cancer: epidemiological considerations and recommendations. Ann Oncol Off J Eur Soc Med Oncol. 2012 Aug;23 Suppl 6:vi7-12.

46. Guo L, Xie G, Wang R, Yang L, Sun L, Xu M, et al. Local treatment for triple-negative

breast cancer patients undergoing chemotherapy: breast-conserving surgery or total mastectomy? BMC Cancer. 2021;21(1):1–12.

47. Michlewska S, Ionov M, Szwed A, Rogalska A, Olmo NS Del, Ortega P, et al. Ruthenium dendrimers against human lymphoblastic leukemia 1301 cells. Int J Mol Sci. 2020;21(11):1–13.

48. Maciel D, Nunes N, Santos F, Fan Y, Li G, Shen M, et al. New insights into ruthenium(ii) metallodendrimers as anticancer drug nanocarriers: from synthesis to preclinic behaviour. J Mater Chem B. 2022;10(43):8945–59.

49. Shcharbin D, Pedziwiatr E, Blasiak J, Bryszewska M. How to study dendriplexes II: Transfection and cytotoxicity. J Control Release. 2010;141(2):110–27.

50. Shcharbin D, Janaszewska A, Klajnert-Maculewicz B, Ziemba B, Dzmitruk V, Halets I, et al. How to study dendrimers and dendriplexes III. Biodistribution, pharmacokinetics and toxicity in vivo. J Control Release. 2014;181(1):40–52.

51. Bae Y, Song SJ, Mun JY, Ko KS, Han J, Choi JS. Apoptin Gene Delivery by the Functionalized Polyamidoamine (PAMAM) Dendrimer Modified with Ornithine Induces Cell Death of HepG2 Cells. Polymers (Basel). 2017;9(6).

52. Dickerson M, Sun Y, Howerton B, Glazer EC. Modifying Charge and Hydrophilicity of Simple Ru(II) Polypyridyl Complexes Radically Alters Biological Activities: Old Complexes, Surprising New Tricks. Inorg Chem. 2014 Oct 6;53(19):10370–7.

53. Koceva-Chyła A, Matczak K, Hikisz MP, Durka MK, Kochel MK, Süss-Fink G, et al. Insights into the in vitro Anticancer Effects of Diruthenium-1. ChemMedChem. 2016 Oct 6;11(19):2171–87.

54. Sanz del Olmo N, Maroto-Diaz M, Quintana S, Gómez R, Holota M, Ionov M, et al. Heterofunctional ruthenium(II) carbosilane dendrons, a new class of dendritic molecules to fight against prostate cancer. Eur J Med Chem. 2020;207.

55. duPre' SA, Hunter KW. Murine mammary carcinoma 4T1 induces a leukemoid reaction with splenomegaly: Association with tumor-derived growth factors. Exp Mol Pathol. 2007;82(1):12–24.

56. Guan X, Li J, Cai J, Huang S, Liu H, Wang S, et al. Iron oxide-based enzyme mimic nanocomposite for dual-modality imaging guided chemical phototherapy and anti-tumor immunity against immune cold triple-negative breast cancer. Chem Eng J. 2021;425(March):130579.

57. Law AMK, Valdes-Mora F, Gallego-Ortega D. Myeloid-Derived Suppressor Cells as a Therapeutic Target for Cancer. Cells. 2020;9(3).

58. Le HK, Graham L, Cha E, Morales JK, Manjili MH, Bear HD. Gemcitabine directly inhibits myeloid derived suppressor cells in BALB/c mice bearing 4T1 mammary carcinoma and augments expansion of T cells from tumor-bearing mice. Int Immunopharmacol. 2009;9(7):900–9.

59. Mebius RE, Kraal G. Structure and function of the spleen. Nat Rev Immunol. 2005;5(8):606–16.

Figure and tables legends

Figure 1. The structures of G1-[[NCPh(o-N)Ru(η6-p- cymene)Cl]Cl]4 (CRD13) and ({[[NCPh(o-N)Ru(η6-p-cymene)Cl]Cl]3[FITC]} (CRD13-FITC).

Figure 2. Scheme of the *in vivo* experimental design. Mice were randomly assigned to 4 independent groups. Mice were inoculated with cancer cells, and from day 2 were treated with **CRD 13** dendrimer for 26 days according to the scheme 2 x 2. Group 1 - NT (PBS), (not treated with **CRD13**, not inoculated with 4T1 cells), Group 2 - (treated with dendrimer every 2 days on the days 2.-28.), Group 3 - (cancer cells application), Group 4 - (inoculated with the cancer cells 4T1+ treatment with the dendrimer every 2 days on the days 2.-28.). Tumours and tissues were collected *post mortem* at day 28 of the experiment.

Figure 3. Viability of EpH4-Ev and 4T1 cells exposed to ruthenium dendrimer **CRD13**. (**A**) – incubation time 24 h, (**B**) – incubation time 72 h. Data, acquired with the use of fluorescence technique, are presented as relative values vs. control samples. Results are shown as raw estimates, means are represented by thick horizontal lines; each point represents the mean of 3 technical replicates of the sample. The significance of differences, as estimated with the bootstrap-boosted two-way ANOVA, was as follows: for EpH4-Ev, the effect of time $P< 0.0001$, for **CRD13** concentration, $P< 0.001$, for the interaction of factors, $P< 0.003$; for 4T1 cells, the effects of time and **CRD13** concentration $P< 0.0001$, for the interaction of factors, $P< 0.001$.

Figure 4*.* Cellular uptake of the FITC-labelled **CRD13**. (**A**) confocal microscopy images; microphotographs taken at λ_{em}=405 and 489 nm, (**B**) fractions of 4T1 cells uptaking **CRD13-FITC**; for the dendrimer concentrations of 10 μg/ml and 20 μg/ml the fractions of labelled cells were, respectively: 5.46+1.21% and 7.46+2.41% for 24 h incubation, and 10.27$\pm$2.13% and 19.64+1.86% for 72 h incubation; the significance by the bootstrap-boosted two-way ANOVA was: for the effects of time and **CRD13** concentration $P< 0.0001$, for the interaction between the factors $P< 0.001$, (**C**) overall fluorescence intensity of **CRD13-FITC** internalized

into the dendrimer-treated cells; for the dendrimer concentrations of 0, 10 μg/ml and 20 μg/ml the fractions of labelled cells were, respectively: 0.183±0.038 a.u., 1.354±0.147 a.u. and 6.309±0.693 a.u; significance by the bootstrap-boosted two-way ANOVA was P< 0.0001 for the effects of time, **CRD13** concentration and the interaction between the factors. The results are shown as the BCA bootstrap-boosted means ± SD of n = 11 (**B**) or n = 12 observations(**C**).

Figure 5. Body and tumour weights. (**A**) The impact of 28-day mice treatment with ruthenium dendrimer on body mass, (**B**) relative mass of the tumour tissue, significance for the relative tumour weight, estimated with the bootstrap-boosted Student t test was *P*< 0.0001, (**C**) the relative spleen weight (spleen mass/ total body mass ratio) of mice; significance, estimated with the bootstrap-boosted two-way ANOVA, was: the effect of the inoculation with 4T1 cells, *P*< 0.0001, for **CRD13** treatment, *P*< 0.02, for the interaction between factors, *P*< 0.025. Dendrimer was applied at the concentration of 10 mg/kg b.w. every day (days 2-28); n = 5 (groups 1 and 2), n = 15 (groups 3 and 4).

Figure 6. Changes of the tumour and spleen weight in mice treated with **CRD13**. (**A**) Tumour images of animals treated or untreated with ruthenium dendrimer **CRD13**. (**B**) tumour weight [mg], thick black horizontal lines stand for means; significance, significance by bootstrap-boosted Student t test, *P*< 0.0001, (**C**) Photographs demonstrating the changes in tumour size under the influence of **CRD13**, (**D**) Spleen images of healthy mice and animals with cancer treated or untreated with **CRD13**, (**E**) spleen weight [mg] in healthy and diseased mice under the influence of **CRD13**; thick black horizontal lines stand for the means; significance by the bootstrap-boosted two-way ANOVA: the effect of inoculation with 1T4 cells, *P*<0.0001, the effect of **CRD13**, *P*< 0.0.04. The dendrimer was applied at the concentration of 10 mg/kg b.w. every 2 days (days 2-28). Group 1 - healthy mice treated with PBS only (control), Group 2 – mice treated with dendrimer, Group 3 – mice inoculated with cancer cells at the day 1 of the experiment, Group 4 – mice applied with cancer cells at the

day 1, and treated with the dendrimer every 2 days on the days 2-28 of the experiment. n = 5 for groups 1 and 2, n = 15 for groups 3 and 4.

Table 1. Inhibition concentrations IC50±SD (μg/ml) resulting in 50% dendrimer-mediated reduction of EpH4-Ev and 4T1 cell viability after 24 h and 72h of incubation.

Table 2. Ruthenium content in the selected organs of mice [$\mu g \cdot g^{-1}$].

Declaration of interests

☒The authors declare that they have no known competing financial interests or personal relationships that could have appeared to influence the work reported in this paper.

☐The authors declare the following financial interests/personal relationships which may be considered as potential competing interests:

Graphical abstract

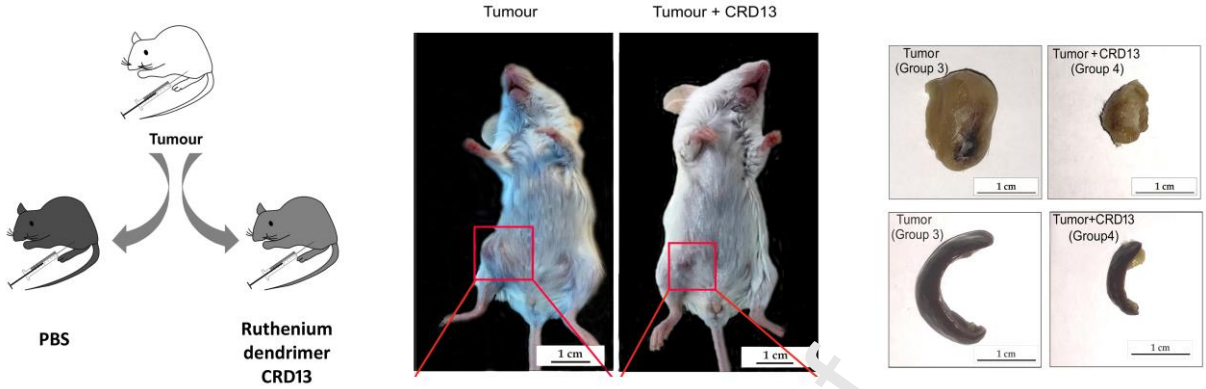

Local injection of ruthenium dendrimer (CRD13) caused significant reduction of tumour mass in mice with triple-negative breast cancer.

Highlights

Carbosilane ruthenium metallodendrimer efficiently entered into the cells, and exhibited selective toxicity for mouse breast cancer cells.

Local injection of ruthenium metallodendrimer caused a reduction of tumour mass in a mouse model with triple-negative breast cancer.

The ICP analyses indicated that Ru(II) accumulated in all tested tissues with a greater content detected in the tumour.